Indoor Air 2005; 15: 291–300
www.blackwellpublishing.com/ina

INDOOR AIR
doi:10.1111/j.1600-0668.2005.00374.x

Novel insight into VOC removal performance of photocatalytic oxidation reactors

Abstract A general model has been developed for analyzing the removal of volatile organic compounds (VOCs) by photocatalytic oxidation (PCO) reactors, taking into consideration of the photocatalytic (surface) reaction and the convective mass transfer coefficients including allowance for their spatial dependence. On this basis, a novel insight into VOC removal performance of PCO reactors is presented. The key parameter for evaluating PCO reactor VOC removal performance is the number of the mass transfer unit (NTU_m), which is shown to be a simple linear product of three dimensionless parameters: the ratio of the reaction area to the cross-sectional area of the flow channel (A^*), the Stanton number of mass transfer (St_m), and the reaction effectiveness (η). The A^* represents the geometric and structural characteristic of a PCO reactor. The St_m shows the synergistic degree of alignment between the fluid and mass flow fields, and reflects the convective mass transfer rate of the reactor. The η, describes the relative intensity between the PCO reaction rate and the mass transfer rate. By using the relationship and the parameters, the influence of various factors on the VOC removal performance, the bottleneck for improving the performance and design of a PCO reactor can be determined. Three examples are used to illustrate the application of our proposed model. It is found that the VOC removal bottleneck is the reaction rate for honeycomb type reactor, while mass transfer rate for light-in-tube type reactor. With six fins the fractional conversion of a light-in-tube reactor increases about 70% relative to the one without any fins.

J. Mo, Y. Zhang, R. Yang
Department of Building Science, Tsinghua University, Beijing, P. R. China

Key words: Photocatalytic oxidation reactor; Volatile organic compounds; Indoor air quality; Convective mass transfer; Field synergy.

Yinping Zhang
Department of Building Science,
Tsinghua University, Beijing 100084,
P. R. China
Tel.: +86 010 6277 2518
Fax: +86 010 6277 3641
e-mail: zhangyp@mail.tsinghua.edu.cn

Received for review 26 November 2004. Accepted for publication 12 April 2005.

Practical Implications
Indoor air quality problem caused by volatile organic compounds (VOCs) have annoyed people for many years. Photocatalytic oxidation (PCO) appears to be a promising technique for destroying VOCs in indoor air. With the model and the novel insight presented in this paper, the influence of various factors on the VOC removal performance can be determined. And the bottleneck for improving the performance of a PCO reactor can be easily identified. These are helpful for designing high performance PCO reactors and optimizing their operative performance.

Introduction

In recent decades, buildings have been sealed more tightly to reduce the energy consumption associated with indoor air-conditioning, meanwhile, with the increasing use of synthetic building materials and furnishings that emit volatile organic compounds (VOCs), the VOC concentrations in indoor air tend to be higher than those allowed by existing codes. High-VOC concentrations indoors have then often been associated with adverse health effects such as allergic reactions; headache; eye, nose or throat irritation; dry cough; dizziness and nausea; difficulty in concentrating and tiredness (Kim et al., 2001; Meininghaus et al., 1999; US EPA, 1990; WHO 1989), which, when taken collectively, is called 'sick building syndrome' (SBS) (Bachmann and Myers, 1995). These symptoms may affect human health severely (Molhave, 1989) and may lead to economic losses (Fisk and Rosenfeld, 1997; Haymore and Odom, 1993). Many advanced technologies for the sustainable environment to quickly and economically remove VOCs from indoor air have been developed by researchers recently. Photocatalytic oxidation (PCO) is an innovative and promising approach among them (Tompkins, 2001).

The VOC removal by PCO is a surface reaction process consisting of two important steps: first, the VOCs have to transfer to the reaction surface; second, the VOCs are decomposed by the photocatalyst. Thus, the VOC convective mass transfer rate, the reaction rate and the reaction surface area are the most important performance parameters of a PCO reactor.

They are affected by many factors such as the reactor geometry, airflow velocity, and the physical properties of VOC species, the wavelength and intensity of the UV irradiation, photocatalyst performances, the temperature of the reaction surface.

Much research has been performed on the way in which these different factors affect the PCO reactor performance (Dreyer et al., 1997; Hall, et al., 1998; Obee and Brown, 1995; Obee, 1996; Obee and Hay, 1997; Yoneyama and Torimoto, 2000). Obviously, it is difficult to know what influence the various factors have on VOC removal performance of PCO reactors only through experiments. Modeling and simulation is a powerful method for determining the relationship of VOC removal performance and the influencing factors. Hossain et al. (1999) developed a three-dimensional convection-diffusion-reaction model for analyzing the VOC removal performance of honeycomb PCO reactors under steady-state conditions, which fitted very well with the experiments. The analysis was impressive. However, the interaction effects between the factors were still not clarified.

Based on a few suitable assumptions, many physical models of PCO reactors were developed. Tronconi and Forzatti (1992) developed a lumped parameter model for a honeycomb structure reactor decomposing NO_x. They derived dimensionless numbers to express the reaction rate and convective mass transfer rate and demonstrated the application of the model to different geometries and boundary conditions. Hall et al. (1998) described a reduced order model for photocatalytic honeycomb reactors, and discussed mass transport and reaction rate limits. He found that the product of volumetric flow rate and conversion rate, which represent the overall rate of VOC removal, reaches an asymptote with the velocity increasing. Zhang et al. (2003) developed a PCO reactor model and found that two parameters, the number of the mass transfer unit, NTU_m, and the fractional conversion, ε were the main parameters influencing the photooxidation performance of a PCO reactor. In the model, it was assumed that the photocatalytic reaction was a first-order reaction with a constant reaction rate coefficient and a constant convective mass transfer coefficient along the flow direction. Based on this model, Yang and Zhang (2004) developed an improved model considering the variable apparent reaction rate coefficient, K, and the variable convective mass transfer coefficient, h_m, along the flow direction. Three new parameters, the ideal reaction number of mass transfer units, $NTU_{m,ir}$, the ideal reaction fractional conversion, ε_{ir},and the reaction effectiveness, η, were defined. The latter is useful in evaluating the upper limit and the bottleneck of VOC removal performance of PCO reactors.

At present, no model has been reported that takes into consideration the variable reaction coefficient of the photocatalytic surface and the convective mass transfer coefficient not only in the axial but also in the perimetric direction. However, almost all the PCO reactors in practice are spatial dependent, especially for the ones with extended surfaces and non-uniform irradiated photocatalytic surfaces with photocatalyst. For example, the radiation distribution on the fins of the light-in-tube type PCO reactor with fins reduces sharply verus the radial direction.

The purpose of the present paper is: (1) to develop a general PCO reactor model that takes account of the variable apparent reaction rate coefficient and convective mass transfer coefficient on the reaction surface (not only in the axial but also in the perimetric direction); (2) to provide a novel insight into the analysis of VOC removal performance of PCO reactors; (3) to determine the relationship between VOC removal performance and the relating factors; (4) to demonstrate the applications of the new model and the relationship by means of examples.

Mechanistic model

In practical applications, three types of PCO reactors (plate, honeycomb, and light-in-tube) are often applied (Figure 1). These reactors can be summarized as shown in Figure 2b, which describes the mass transfer balance of a finite element in the cross-section. A general model will be developed for these prototypical PCO reactors.

The following assumptions are made: (1) the cross-sectional shape remains the same along the airflow direction; (2) there is only one species of VOC in indoor air or the VOCs can be treated as one species.

To simplify the analysis, the photocatalytic reaction rate is expressed as the product of the VOC concentration adjacent to the reaction surface and the apparent reaction rate coefficient. Thus, for the PCO reactor shown in Figure 2b, the mass conservation equation and boundary condition can be written as

$$-G\frac{\mathrm{d}C(z)}{\mathrm{d}z} = \int_{L_\xi} r(z,\xi)\mathrm{d}\xi \tag{1}$$

$$r(z,\xi) = K(z,\xi)C_S(z,\xi) = h_m(z,\xi)(C(z) - C_S(z,\xi)) \tag{2}$$

$$z = 0, \quad C(z) = C_{in} \tag{3}$$

where z is the distance in the axial direction, m; ξ is the distance in the perimetric direction, m; L is the length of the channel, m; L_ξ is the perimeter of the cross-sectional area of the reaction surface path, m; G is the volumetric airflow rate, m^3s; $C(z)$ is the mass-rate-averaged VOC concentration on the cross-section at location z, i.e.:

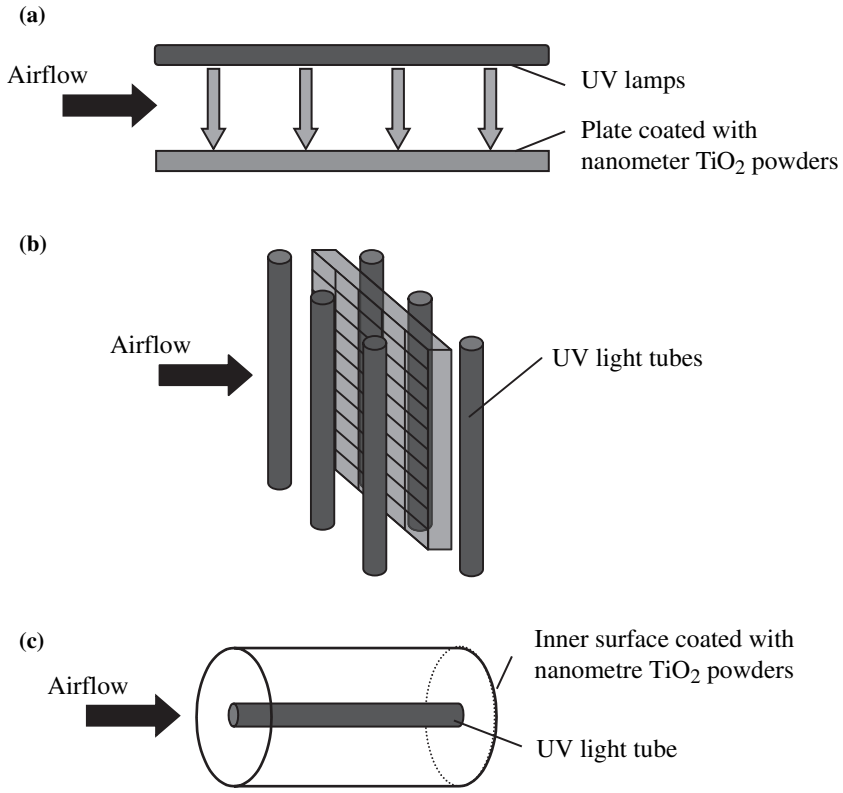

Fig. 1 Schematic of several PCO reactors: (a) plate type reactor; (b) honeycomb type reactor; (c) light-in-tube reactor

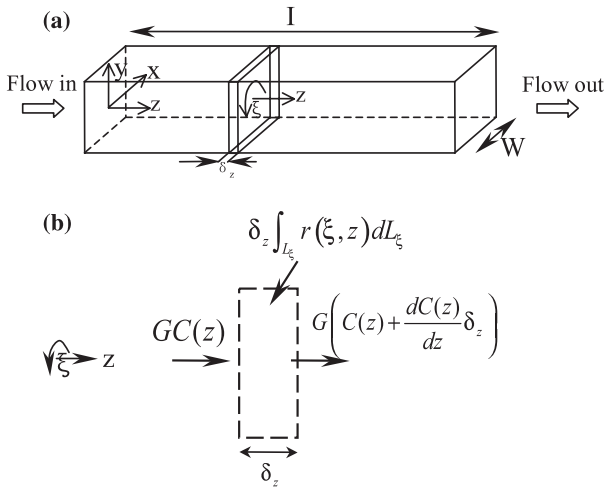

Fig. 2 Schematic of a channel of a monolith PCO reactor: (a) coordinates of the channel; (b) mass balance of the finite cross-sectional element

$$C(z) = \frac{\int_{A_c} (uC)\mathrm{d}A_c}{\int_{A_c} u\mathrm{d}A_c} \tag{4}$$

where u is the velocity compound in z direction, A_c is the cross-sectional area, m^2; $C_s(z, \xi)$ is the local VOC concentration in the air adjacent to the air-solid interface at location (z, ξ), mol/m^3;C_{in} is the inlet VOC concentration, mol/m^3; $r(z, \xi)$ is the local reaction rate at location (z, ξ), $mol/m^2/s$; $K(z, \xi)$ is the local apparent reaction rate coefficient at location (z, ξ), m/s, which is the function of intensity and wavelength of UV light, the physical properties of photocatalyst, the humidity concentration and VOC concentration (based on the Langmuir–Hinshelwood kinetic rate formula in Obee, 1996); and $h_m(z, \xi)$ is the local convective mass transfer coefficient at location (z, ξ), m/s.

Defining the local total VOC removal factor:

$$K_t(z, \xi) = \frac{1}{1/K(z, \xi) + 1/h_m(z, \xi)} \tag{5}$$

the solution of Equation 1 gives

$$\ln C_{out} - \ln C_{in} = -\frac{1}{G}\int_0^L \int_0^{L_\xi} K_t(z, \xi)\mathrm{d}\xi\mathrm{d}z \tag{6}$$

where C_{out} is the outlet VOC concentration, mol/m^3.

Define the average total VOC removal factor K_t as follows:

$$K_t = \frac{\int_0^L \int_0^{L_\xi} K_t(z, \xi)\mathrm{d}\xi\mathrm{d}z}{\int_0^L \int_0^{L_\xi} \mathrm{d}\xi\mathrm{d}z} = \frac{\int_0^L \int_0^{L_\xi} K_t(z, \xi)\mathrm{d}\xi\mathrm{d}z}{A_r} \tag{7}$$

where A_r is the reaction surface area, m^2. Combining Equations 6 and 7 yields

$$C_{out} = C_{in}e^{-(K_t A_r/G)} \tag{8}$$

The number of the mass transfer unit, NTU_m, the fractional conversion, ε, and removal rate, $\dot{m}$ for a PCO reactor are expressed as follows:

$$NTU_m = \frac{K_t A_r}{G} \tag{9}$$

$$\varepsilon = \frac{C_{in} - C_{out}}{C_{in}} = 1 - e^{-NTU_m} \tag{10}$$

$$\dot{m} = G\varepsilon = G(1 - e^{-NTU_m}) \tag{11}$$

When $h_m(z, \xi)$ and $K(z, \xi)$ are independent of location ξ, this model can be simplified to the model of Yang et al. (2004); when independent of both z and ξ, this model can be simplified to the model of Zhang et al. (2003). The advantage of the present model is that it can be used to analyze the VOC removal performance of three-dimensional PCO reactors, in particular to those with inner extended surfaces and spatially dependent mass transfer rate coefficient and reaction rate coefficient.

From Equation 9, the fractional conversion, ε, monotonically increases with increasing NTU_m. Thus, in order to improve fractional conversion of a PCO reactor, it is very important to analyze how to increase NTU_m.

Novel insight into VOC removal performance of PCO reactors

Novel insight into the number of the mass transfer unit, NTU_m

NTU_m can be rewritten as follows:

$$NTU_m = \frac{K_t A_r}{G} = \frac{K_t A_r}{u_a A_c} = \frac{1}{A_c}\int_0^L \int_0^{L_\xi} \frac{1/u_a}{1/K(z,\xi) + 1/h_m(z,\xi)} d\xi dz \tag{12}$$

where u_a is the average air velocity of the cross-sectional flow area, m/s.

Applying the Reynolds number, Re; Schmidt number, Sc; local Sherwood number, $Sh(z, \xi)$; local Damkohler number (Tronconi and Forzatti, 1992), $Da(z, \xi)$:

$$Re = \frac{u_a d_e}{v}, \qquad Sc = \frac{v}{D}$$
$$Sh(z,\xi) = \frac{h_m(z,\xi) d_e}{D} \tag{13}$$
$$Da(z,\xi) = \frac{K(z,\xi) d_e}{D}$$

we have

$$NTU_m = \frac{1}{A_c}\int_0^L \int_0^{L_\xi} \left(\frac{Sh(z,\xi)}{ReSc}\frac{1}{Sh(z,\xi)/Da(z,\xi) + 1}\right) d\xi dz \tag{14}$$

where d_e is the equivalent diameter of the air flow channel, m; v is the kinematic viscosity, m^2/s; and D is the diffusion coefficient of the VOC species in air, m^2/s.

Applying the local Stanton number of mass transfer:

$$St_m(z,\xi) = \frac{Sh(z,\xi)}{ReSc} \tag{15}$$

and defining the local reaction effectiveness:

$$\eta(z,\xi) = \frac{1}{Sh(z,\xi)/Da(z,\xi) + 1} \tag{16}$$

Equation 14 can be rewritten as:

$$NTU_m = \frac{1}{A_c}\int_0^L \int_0^{L_\xi} St_m(z,\xi)\eta(z,\xi) d\xi dz \tag{17}$$

The average St_m and η for the whole reactor can be expressed as follows:

$$St_m = \frac{\int_0^L \int_0^{L_\xi} St_m(z,\xi) d\xi dz}{\int_0^L \int_0^{L_\xi} d\xi dz} = \frac{\int_0^L \int_0^{L_\xi} St_m(z,\xi) d\xi dz}{A_r} \tag{18}$$

$$\eta = \frac{\int_0^L \int_0^{L_\xi} (St_m(z,\xi)\eta(z,\xi)) d\xi dz}{\int_0^L \int_0^{L_\xi} St_m(z,\xi) d\xi dz} = \frac{\int_0^L \int_0^{L_\xi} (St_m(z,\xi)\eta(z,\xi)) d\xi dz}{A_r St_m} \tag{19}$$

We then have

$$NTU_m = A^* St_m \eta$$
$$A^* = \frac{A_r}{A_c} \tag{20}$$

where A^* is the area ratio of the reaction area to the cross-sectional area. Clearly, NTU_m is the linear product of three parts, A^*, St_m, and η.

Applying the Taylor series yields:

$$(1 - e^{-NTU_m}) = \sum_{n=1}^{\infty} (-1)^{n-1} \frac{(NTU_m)^n}{n!} = \sum_{n=1}^{\infty} (-1)^{n-1} \frac{(A^* St_m \eta)^n}{n!} \tag{21}$$

Thus, the VOC removal rate is expressed as

$$\dot{m} = G\varepsilon = u_a A_c \sum_{n=1}^{\infty} (-1)^{n-1} \frac{(A^* St_m \eta)^n}{n!} = A_r h_m \eta - \frac{(A_r h_m \eta)^2 (u_a A_c)^{-1}}{2!} + \frac{(A_r h_m \eta)^3 (u_a A_c)^{-2}}{3!} \cdots \quad (22)$$

If u_a is high enough

$$\dot{m} \approx A_r h_m \eta \quad (23)$$

Therefore, when the averaged velocity, u_a, increases, at some point $\dot{m}$ reaches an asymptote, which is accordant with Hall's conclusion (Hall et al., 1998). Furthermore, the limit value of $\dot{m}$ is a linear product of A_r, h_m, and η.

In summary, the VOC removal performance of PCO reactors improves with increasing values of the aforementioned dimensionless parameters. Applying this model, the influence of geometry and configuration, convective mass transfer rate and PCO reaction rate etc. on the VOC removal performance of a PCO reactor can be analyzed.

Novel insight into St_m: analysis of synergy of flow and mass fields

St_m is a dimensionless mass transfer parameter. We find that it shows the synergistic degree of fluid and mass flow fields. The field synergy between flow and heat transfer was analyzed by Guo et al (1998, 2001), based on the parabolic fluid flow. Tao et al. (2002, 2002) extended the concept to elliptic fluid flow and other heat transfer problems. This concept was well used in heat transfer enhancement, but not in mass transfer field. Similarly, from the analogy between heat transfer and mass transfer, the synergy of fluid and mass flow fields presents a new insight into the physical meaning of St_m. Based on Guo's concept, this section will derive how to enhance the mass transfer.

For two-dimensional steady boundary flow, the mass balance equation is written as

$$u\frac{\partial C}{\partial x} + v\frac{\partial C}{\partial y} = D\frac{\partial^2 C}{\partial y^2} \quad (24)$$

where x is the coordinate along the flow, and y that normal to x; u and v are the velocity components in x and y directions, respectively, m/s; C is mole concentration, mol/m^3.

Integrating Equation 24 in the boundary layer and combining the definition of convective mass transfer coefficient yields:

$$h_m(x) = \frac{\int_0^{\delta_m(x)} \left(u\frac{\partial C}{\partial x} + v\frac{\partial C}{\partial y}\right) dy}{C_s(x) - C_\infty} = u_\infty \frac{\int_0^{\delta_m(x)} \left(u\frac{\partial C}{\partial x} + v\frac{\partial C}{\partial y}\right) dy}{\int_0^{\delta_m(x)} \left(0\frac{\partial C}{\partial x} - u_\infty \frac{\partial C}{\partial y}\right) dy} \quad (25)$$

where $\delta_m(x)$ is the mass boundary layer thickness at x location, m, and the subscript, w, stands for wall; C_∞ is the VOC mole concentration in free-stream flow, mol/m^3; $C_s(x)$ is the VOC mole concentration in the air adjacent to the surface at y location, mol/m^3.

Defining the vector:

$$\mathbf{U}_\infty = 0\mathbf{i} - u_\infty \mathbf{j} \quad (26)$$

and the following dimensionless variables:

$$\bar{\mathbf{U}} = \frac{\mathbf{U}}{u_\infty}, \quad \bar{\mathbf{U}}_\infty = \frac{\mathbf{U}_\infty}{u_\infty}, \quad \bar{x} = \frac{x}{\delta_m(x)}, \quad \bar{y} = \frac{y}{\delta_m(x)}, \quad \nabla\bar{\mathbf{C}} = \frac{\nabla \mathbf{C}}{(C_S(x) - C_\infty)/\delta_m(x)} \quad (27)$$

We then have

$$Sh(x) = \frac{h_m(x) l}{D} = \frac{u_\infty l}{v}\frac{v}{D}\frac{\int_0^1 (\bar{\mathbf{U}} \cdot \nabla\bar{\mathbf{C}}) d\bar{y}}{\int_0^1 (\bar{\mathbf{U}}_\infty \cdot \nabla\bar{\mathbf{C}}) d\bar{y}} = Re\ Sc \frac{\int_0^1 (\bar{\mathbf{U}} \cdot \nabla\bar{\mathbf{C}}) d\bar{y}}{\int_0^1 (\bar{\mathbf{U}}_\infty \cdot \nabla\bar{\mathbf{C}}) d\bar{y}} \quad (28)$$

where '·' refers to the dot product, and Δ is the gradient operator; u_∞ is free-stream fluid velocity, m/s; l stands for the characteristic length, m; Sh, Re, and Sc represent the Sherwood number, the Reynolds number and the Schmidt number, respectively. The vector dot product in Equation (28) can be expressed as:

$$\bar{\mathbf{U}} \cdot \nabla\bar{\mathbf{C}} = |\bar{\mathbf{U}}||\nabla\bar{\mathbf{C}}| \cos\beta, \quad \bar{\mathbf{U}}_\infty \cdot \nabla\bar{\mathbf{C}} = |\bar{\mathbf{U}}_\infty||\nabla\bar{\mathbf{C}}| \cos\beta_\infty \quad (29)$$

where $\beta(\beta_\infty)$ is the intersection angle between $\bar{\mathbf{U}}(\bar{\mathbf{U}}_\infty)$ and $\Delta\mathbf{C}$. In most practical problems, in the concentration boundary layer, there is $\frac{\partial C}{\partial y} \gg \frac{\partial C}{\partial x}$. Therefore, β_∞ is close to zero. So Equation 28 can be rewritten as

$$St_m(x) = \frac{Sh(x)}{Re\ Sc} = \frac{\int_0^1 (|\bar{\mathbf{U}}||\nabla\bar{\mathbf{C}}|) d\bar{y}}{\int_0^1 (|\nabla\bar{\mathbf{C}}|) d\bar{y}} \quad (30)$$

It is evident from Equation 30 that: (1) St_m depends not only on the values of the velocity and concentration gradient of fluid flow, but also on the intersection angle between them; (2) $St_m \leq 1$, only when there is $|\mathbf{U}| = 1$ and $\beta = 0$ everywhere, $St_m = 1$, that is, the vector $\bar{\mathbf{U}}$ has to be the same with $\bar{\mathbf{U}}_\infty$, not only the value but also the vector direction; Obviously, when $\beta = 0$ everywhere, $|\bar{\mathbf{U}}|$ must be equal to 1; (3) β plays an important role in describing the synergistic degree of fluid and mass flow fields.

For three-dimensional steady flow and mass transfer problems, the mass balance equation is written as

$$\vec{\mathbf{U}} \cdot \nabla C = \nabla \cdot (D\nabla C) \quad (31)$$

where $\vec{\mathbf{U}}$ is the velocity vector, and ∇ is the divergence operator.

Integrated over the whole field, Equation 31 is rewritten as

$$\int_{\mathbf{V}} (\vec{\mathbf{U}} \cdot \nabla C) \mathrm{d}V = \int_{\mathbf{V}} (\nabla \cdot (D \nabla C)) \mathrm{d}V = \int_{\mathbf{S}} (\vec{\mathbf{n}} \cdot (D \nabla \mathbf{C})) \mathrm{d}S \tag{32}$$

where V is the whole field volume, m^3, with a bounding surface S, m^2; $\vec{\mathbf{n}}$ is the unit vector normal to the boundary, S. Further derivation of Equation 32 yields:

$$\int_{\mathbf{V}} (|\vec{\mathbf{U}}||\nabla C| \cos\beta) \mathrm{d}V = \int_{\mathbf{S}} (\vec{\mathbf{n}} \cdot (D \nabla \mathbf{C})) \mathrm{d}S \tag{33}$$

The average value of $(|\vec{\mathbf{U}}||\nabla C|)$, and the average intersection angle are defined as follows:

$$(|\vec{\mathbf{U}}||\nabla C|)_{\mathrm{a}} = \frac{\int_{\mathbf{V}} (|\vec{\mathbf{U}}||\nabla C|) \mathrm{d}V}{\int_{\mathbf{V}} \mathrm{d}V} = \frac{\int_{\mathbf{V}} (|\vec{\mathbf{U}}||\nabla C|) \mathrm{d}V}{V} \tag{34}$$

$$\cos\beta_{\mathrm{a}} = \frac{\int_{\mathbf{V}} (|\vec{\mathbf{U}}||\nabla C| \cos\beta) \mathrm{d}V}{\int_{\mathbf{V}} (|\vec{\mathbf{U}}||\nabla C|) \mathrm{d}V} = \frac{\int_{\mathbf{S}} (\vec{\mathbf{n}} \cdot (D \nabla \mathbf{C})) \mathrm{d}S}{(|\vec{\mathbf{U}}||\nabla C|)_{\mathrm{a}} \cdot V} \tag{35}$$

From Equation 35, it is seen that if the integral value $\left(\int_{\mathbf{S}} (\vec{\mathbf{n}} \cdot (D \nabla \mathbf{C})) \mathrm{d}S\right)$ is positive, β_{a} is in the range of $0 - \pi/2$; if the integral value is minus, β_{a} is in the range of $\pi/2 - \pi$. When $\beta_{\mathrm{a}} = \pi/2$, the integral value $\left(\int_{\mathbf{S}} (\vec{\mathbf{n}} \cdot (D \nabla \mathbf{C})) \mathrm{d}S\right)$ is null, which means that the mass flux on the reaction surface is zero. Thus, the fractional conversion of the reactor is 0%. If $\beta_{\mathrm{a}} = 0$ (or π), $St_{\mathrm{m}} = 1$, which means that $\mathrm{NTU_m}$=A*1η. Thus, in this case, the fractional conversion depends only on A* and η.

β_{a} is important to analyzing the value of St_{m}. The average St_{m} is proportional to the cosine value of the average angle. For example, if the average angle reduces from 89 to 88°, the cosine value of the average angle increases about 100%.

Discussion on A*, St_{m}, and η

*Discussion on A**. A* is a very useful parameter in optimizing a PCO reactor geometric configuration. Considering that $0 \le \eta \le 1$ and $0 \le St_{\mathrm{m}} \le 1$, the maximal value of $\mathrm{NTU_m}$ is A*, theoretically. If taking $\mathrm{NTU_m}$ as A*, the fractional conversion is still not satisfactory, it means that no matter how much the mass transfer and reaction rate are enhanced, the VOC removal performance cannot reach the desired level. For this case, the geometric configuration design or selection should not be accepted.

Therefore, A* can be regarded as a reactor geometric configuration evaluation parameter with which any unreasonable reactor geometric design or selection can easily be found.

Discussion on St_m. The mass transfer is the precondition of a PCO reaction. That is to say, it has to make sure that the mass transfer rate is high enough to guarantee the high reaction rate. If the value of A* is high enough, the value of St_{m} will determine the VOC removal performance. Assuming $\eta = 1$, the maximal value of $\mathrm{NTU_m}$ is (A^* St_{m}). Only when the value of (A^* St_{m}) is high, the VOC removal performance of the reactor is promising. Otherwise the reactor design is failed. Therefore, St_{m} can be regarded as the mass transfer evaluation parameter with which the mass transfer bottleneck of any unreasonable reactor can be found. From Equation 31, it is known that adjusting the airflow direction normal to the reaction surface may enhance St_{m}.

From Equation 30 and the definition of the convective mass transfer coefficient, it yields:

$$St_{\mathrm{m}} = \frac{h_{\mathrm{m}}}{u_{\mathrm{a}}} = -D \frac{\nabla C|_{\mathrm{wall}}}{(C_{\mathrm{m}} - C_{\mathrm{S}})} \frac{1}{u_{\mathrm{a}}} \tag{36}$$

where $\nabla C|_{\mathrm{wall}}$ is the concentration gradient on the reaction surface; C_{m} is the mass-rate-averaged concentration of the cross-sectional area. Thus, if the term ($\nabla C|_{\mathrm{wall}}/C_{\mathrm{m}} - C_{\mathrm{S}}$) is not equal to constant (as is the case in most practical situations), St_{m} is the function of the concentration distribution. Tronconi and Forzatti (1992) found that the Sherwood number, Sh, vary with the value of the Damkohler number, Da. That is to say, St_{m} depends on η. Thus, it implies that η influences the concentration distribution, and then affects St_{m}, indirectly.

However, if the VOC concentration difference in the PCO reactor is not high, the influence of VOC concentration to St_{m} can be neglected, just as the situation of the influence of temperature to the heat transfer. Zhang et al. (2003) found that when the VOC concentration is low (lower than 2 ppmv), $\mathrm{NTU_m}$ remains almost constant in a series of experiments with various VOC concentrations. Therefore, it is justified to assume that St_{m} is independent of the VOC concentration if the concentration is low (as is the case in most practical situations).

Discussion on $\eta(z, \xi)$ and η. If the value of (A^* St_{m}) is satisfactory, the value of η will determine whether the reactor is available or not.

Equation 16 can be changed into

$$\eta(z, \xi) = \frac{1}{h_{\mathrm{m}}(z, \xi)/K(z, \xi) + 1} \tag{37}$$

If the mass transfer rate is much greater than the reaction rate, i.e. $h_m(z, \xi) \gg K(z, \xi)$, $\eta(z, \xi)$ approaches its minimum, 0. If the reaction rate is much greater than the mass transfer rate, i.e. $K(z, \xi) \gg h_m(z, \xi)$,$\eta(z, \xi)$ approaches its maximum, 1. Therefore, η, the averaged value of $\eta(z, \xi)$ for the whole reaction surface, can be regarded as a PCO reaction evaluation parameter. If η is near 0, it implies that the bottleneck of VOC removal by a PCO reactor is reaction rate. For this case, applying a high performance photocatalyst or improving the reaction condition may obviously increase VOC removal performance.

Determination of A^*, St_m, η, and β_a for a given PCO reactor

A^* can be calculated by the geometric size of the PCO reactor. St_m can be calculated by using the Computational Fluid Dynamic (CFD) method or by using suitable empirical correlations. NTU_m is calculated by using the measured fractional conversion, ε of a PCO reactor. When A^*, St_m, and NTU_m are known, η can be calculated by using Equation 20. In addition, η also can be calculated by using Equation 19 and CFD method.

If applying the CFD method, the velocity field and the concentration gradient of VOC within the PCO reactor can be determined. Thus, the parameter, β_a can be calculated out by using Equation 35.

Illustrative examples

In order to illustrate the applications of NTU_m, A^*, St_m, η, and β_a for analyzing VOC removal performance by a PCO reactor, the following examples are presented.

Influence of β_a on St_m: mass transfer between two semi-infinite plates

Consider the problems shown in Figure 3: (a) fully-developed mass flow and laminar flow with average u_a inside two parallel plates; (b) laminar flow with uniform velocity, u_a, normal to two parallel porous plates [these two cases are similar to Guo's illustrations (Guo, 2001).

In these two cases, the bottom porous plates are kept at uniform VOC concentration, $C_1 > 0$; the top porous plates are coated with nanometer TiO_2 powders in the inner surfaces, with UV lamps irradiating from outsides. Adjust the UV light intensity to keep a very low VOC concentration on the inner surfaces of the top plates, $C_2 \approx 0$.

Case a. In the fully developed mass and laminar flow, we have

$$\partial u/\partial x = 0, \quad v = 0, \quad \partial C/\partial x = 0, \quad \partial^2 C/\partial y^2 \geq \partial^2 C/\partial x^2 \tag{38}$$

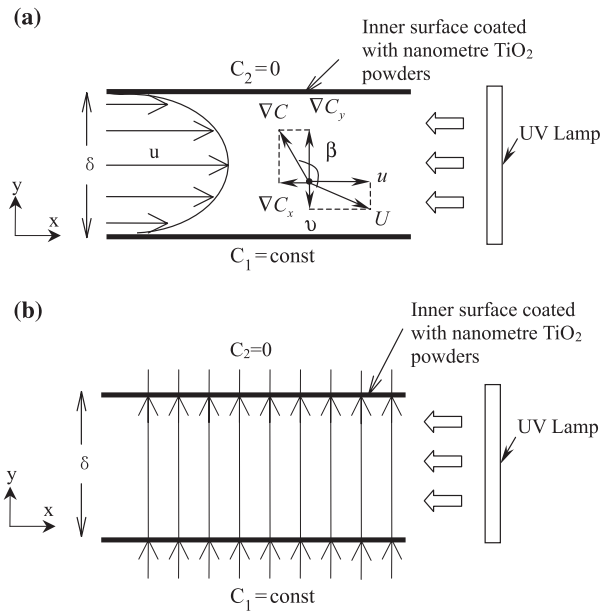

Fig. 3 Schematic of laminar flows between two parallel plates: (a) fully developed flow parallel to the plates; (b) uniform flow normal to the plates.

The mass equation can be simplified as

$$\frac{\partial^2 C}{\partial y^2} = 0 \tag{39}$$

It is subjected to the boundary conditions:

$$C(0) = C_1, \qquad C(\delta) = 0 \tag{40}$$

The analytical solution of Equation 39 gives

$$C = -\frac{C_1}{\delta} y + C_1 \tag{41}$$

In this case the concentration gradient is normal to the plates but the velocity parallel, i.e., $v = 0$, $\partial C/\partial x = 0$ (Figure 3a). The intersection angle β between U and ∇C is always equal to $\pi/2$. For the top plate:

$$Sh = 1, \qquad St_m = \frac{Sh}{Re\ Sc} = \frac{1}{Re\ Sc} \tag{42}$$

where $Re = u_a\delta/v$. Usually, Sc is near 1 for gas phase VOC, and Re is much greater than 1. Thus, St_m tends to be much less than 1 in this case.

Case b The mass equation can be simplified as

$$u_a \frac{dC}{dy} = D \frac{d^2 C}{dy^2} \tag{43}$$

It is subjected to the boundary conditions:

$$u(0) = u_a, u(\delta) = u_a; \quad C(0) = C_1, C(\delta) = 0 \tag{44}$$

The analytical solution of Equation 43 is

$$C = \frac{-C_1}{e^{Re\ Sc} - 1}\left(e^{\frac{Re\ Sc}{\delta}y} - 1\right) + C_1 \tag{45}$$

In this case the concentration gradient and the velocity are both parallel to the plates, i.e. the intersection angle between U and ∇C always equals to 0.

For the top plate, we have

$$St_m = \frac{\exp(Re\ Sc)}{\exp(Re\ Sc) - 1} \tag{46}$$

Usually, due to that $Re\ Sc$ is much greater than 0, St_m is close to its maximum, 1.

In summary, the intersection angle between concentration gradient and velocity plays a key role in the mass transfer process. As well known, for the typical PCO reactor, the airflow usually flows along the reaction surface in parallel, which results in

$$v \ll u, \qquad \frac{\partial C}{\partial x} \ll \frac{\partial C}{\partial y} \tag{47}$$

That is the reason why β is close to $\pi/2$ (Figure 3a). In order to enhance the mass transfer rate, it is necessary and effective to increase the velocity normal to the reaction surface (Figure 3b).

Honeycomb type reactors

Hossain et al. (1999) developed a mathematical model to describe the VOC removal performance of a titania-coated honeycomb monolith PCO reactor for air purification (Figure 1b). In the experiment, they employed two-monolith/one-UV-lamp-bank configuration. Monolith lengths were 0.5, 1.0, and 1.5 in. (12.7, 25.4, and 38.1 mm). Each monolith contained 64 cells per square inch (CPSI). The flow rate was 55 cubic feet per min (CFM), with mean UV intensities on the 12×12 in. monolith face of 6.5 mW/cm^2. The inlet formaldehyde concentration was 2.1 ppmv and the water concentration was 2700 ppmv.

Applying Hossain's model, we solved the conservation equations, including the convection, diffusion and reaction for each component in the monolith, using Phoenics 3.3 (Commercial CFD software). The coordinate system is shown in Figure 2a, with the transverse coordinates x and y, and the axial coordinate z. A uniform mesh with fixed step size of 0.1 mm was used for the full domain of the channel. Numerical 'experiments' were carried out to ensure the independence of the results on the mesh and error tolerances. Use of the mesh with a step size of 0.05 mm and more stringent error tolerances had no significant effect on the solution. Thus, NTU_m, A^*, St_m, η, and β_a were obtained by using Equations 18–20 and 35.

Table 1 lists the CFD-simulated and experimental results for the formaldehyde conversion tests. Compared with Hossain's experimental data, a statistical best-fit result was obtained, with a slope of 1.045, R^2 of 0.972. Thus, the CFD method is capable of predicting the experimental results with a high level of confidence.

If the acceptable value for the fractional conversion is 85%, the NTU_m value should be greater than 2 (see Equation 9). According to the discussion in 'Discussion on A^*, St_m, and η,' the VOC removal performance can be evaluated step by step. From Table 1, it is known that A^* values are always much greater than 1. Thus, the geometry design for this type PCO reactor is satisfactory. In addition, the products ($A^*\ St_m$) are also greater than 2 except for Test 1. However, the final fractional conversions are less than 85% because of low η values. It implies that the bottleneck for honeycomb type PCO reactor is the reaction rate. From Hossain's paper (1999), it is known that the UV radiation intensity drops sharply with increasing distance into the channel. This is the main reason for a small value of η.

From Table 1, it is also seen that St_m is much smaller than its maximum, 1. Figure 4 shows the intersection angle distribution at the plane of $X = 0.5$. The intersection angle, β, is close to 90°, especially on the reaction surface ($Y = 1$). Therefore, the averaged intersection angles, β_a, approaches 90°(see Table 1), resulting in low St_m values. Hence, for this typical PCO reactor (see discussion in 'Influence of β_a on St_m: mass transfer between two semi-infinite plates'), A^* offsets the low St_m values which makes the product ($A^*\ St_m$) satisfactory.

Table 1 The simulated and experimental results for formaldehyde removal

Test	Lamp number/number of surface radiated	Monolith length (in.)	Measured ε (%)	Simulated ε (%)	Diff. (%)	$\dot{m} = G\varepsilon$ ($\times 10^{-3}$ m^3/h)	NTU_m ($\times 10^{-1}$)	A^*	St_m ($\times 10^{-2}$)	η (%)	β_a (degree)
1	4/1	0.5	35.0	36.1	−3.17	3.32	4.48	16.0	9.67	29.0	98.0
2	4/2	0.5	52.5	57.4	−9.35	5.28	8.53	32.0	7.73	34.5	95.4
3	4/1	1.0	42.5	40.5	4.80	3.73	5.18	32.0	7.73	21.0	96.9
4	4/2	1.0	60.5	64.2	−6.12	5.91	10.30	64.0	6.90	23.3	95.6
5	4/1	1.5	43.5	46.4	−6.55	4.27	6.23	48.0	7.18	18.1	95.1
6	4/2	1.5	66.0	68.3	−3.50	6.28	11.50	96.0	6.66	18.0	94.9

The airflow rate for the tests above is about 0.0092 m^3/h.

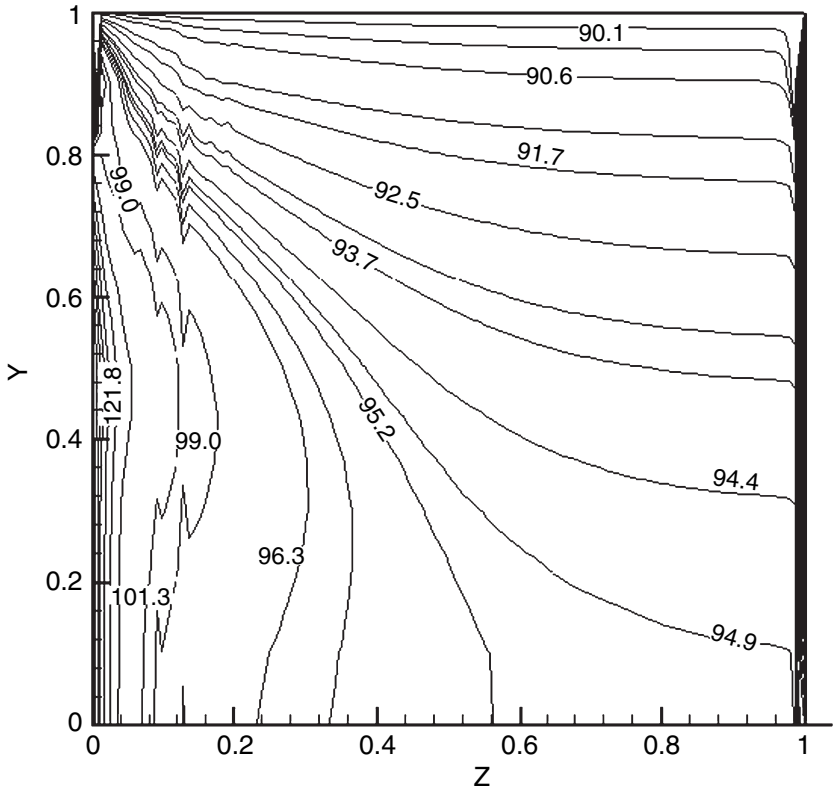

Fig. 4 Intersection angle distribution at the plane of dimensionless $X = 0.5(X = x/W,\ Y = y/W,\ Z = z/L)$.

Light-in-tube type reactors

The formaldehyde removal performances of two kinds of light-in-tube PCO reactors designed by us were measured in a gas-tight stainless steel chamber, $1.2 \times 1.2 \times 1.2$ m^3, with no VOC emission sources and sinks. By using a gas analyzer (INNOVA 1312) and a data log system, the fractional conversion, ε, is evaluated based on the method developed by Zhang et al. (2003). The VOC removal performance is simulated by, using CFD method introduced in the section for honeycomb type PCO reactors.

Table 2 lists the formaldehyde removal performances of the two light-in-tube reactors: without fins (Figure1c) and with six fins coated with nanometer TiO_2 powder, P25 (Figure 5). The inner diameter and the length of the tubes are 48 mm and 26.5 cm, respectively. The UV lamp's external diameter is 15 mm with the same length as the tube, and its irradiative wavelength is 254 nm with UV intensities from the lamp surface, 4.54 mW/cm^2. The air volumetric flow rate through the tube is 25.0 m^3/h. In the gas-tight chamber, the air temperature and relative humidity (RH) are controlled at 25°C and 50%, respectively. The initial formaldehyde concentration in the test chamber is 1.50 ppmv.

Using the same evaluating method discussed in the section for honeycomb type reactor, it is known that

Table 2 The formaldehyde removal performances of the two light-in-tube reactors: without fins and with fins

PCO reactor	ε (%)	$\dot{m} = G\varepsilon$ (m^3/h)	NTU_m ($\times 10^{-2}$)	A^*	St_m ($\times 10^{-3}$)	η (%)	β_a (degree)
Without fins	5.42	1.36	5.57	24.5	2.97	76.6	90.0
With six fins	9.40	2.35	9.87	56.6	3.20	54.7	90.1

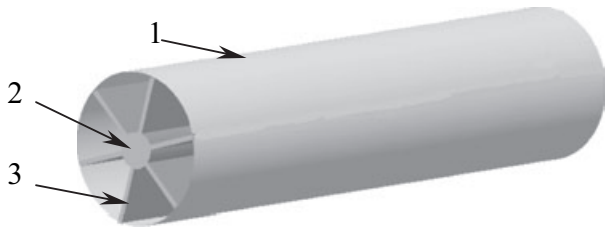

Fig. 5 Schematic of the light-in-tube PCO reactor with six fins. 1, steel tube whose inner surface is coated with nanometer TiO_2 powder; 2, UV lamp; 3, fins coated with nanometer TiO_2 powder on both sides.

A^* and η are both large enough. However, but St_m is not satisfactory because the product of (A^* St_m) is quite small. Compared with honeycomb type reactor, η for light-in-tube PCO reactor is greater but St_m is

smaller. It implies that the VOC removal bottleneck for light-in-tube type PCO reactor is the mass transfer rate.

With six fins, St_m increases a little and A^* obviously increases. Although η decreases, NTU_m increases more than 70% relative to the one without any fins.

Conclusions

- A general model is developed for analyzing VOC removal performance of PCO reactors, taking into consideration the spatially dependent reaction coefficient of photocatalytic surfaces and the convective mass transfer coefficient.
- A novel insight into the number of the mass transfer unit, NTU_m, shows that it is a simple linear product of three-dimensionless parameters: A^*, St_m, and η. By using the relationship and the parameters, the influence of various factors on the VOC removal performance of a PCO reactor can be determined.
- The dimensionless mass transfer number, St_m, is the parameter describing the synergistic degree of fluid flow and concentration fields. It depends not only on the velocity, concentration distributions and physical properties of fluid flow and the species in it, but also on the intersection angle between fluid flow and concentration fields. The averaged intersection angle, β, plays an important role in describing the synergistic degree of fluid and mass flow fields. Increasing the velocity normal to the reaction surface can enhance the mass transfer.
- η describes the relative intensity between the PCO reaction rate and the mass transfer rate, which clearly shows PCO reaction performance of a reactor. If η is near 0, it implies that the bottleneck of VOC removal of a PCO reactor is reaction rate.
- The relationship between NTU_m, A^*, St_m, and η, and their associated parameters are very useful in PCO reactor design and performance evaluation.

Acknowledgements

This work was supported by the National Nature Science Foundation of China (Grant Nos: 50276033 and 50436040).

References

Bachmann, M.O. and Myers, J.E. (1995) Influences on sick building syndrome symptoms in three buildings, *Soc. Sci. Med.*, **40**, 245–251.

Dreyer, M., Newman, G.K., Lobban, L., Kersey, S.J., Wang, R. and Harwell, J.H. (1997) Enhanced oxidation of air contaminants on an ultra-low density UV-accessible aerogel photocatalyst, *Mater. Res. Soc. Symp. Proc.*, **454**, 141–146.

Fisk, W.J. and Rosenfeld, A.H. (1997) Estimates of improved productivity and health from better indoor environments, *Indoor Air*, **7**, 158–172.

Guo, Z.Y., Li, D.Y. and Wang, B.X. (1998) A novel concept for convective heat transfer enhancement, *Int. J. Heat Mass Transfer*, **41**, 2221–2225.

Guo, Z.Y. (2001) Mechanism and control of convective heat transfer –coordination of velocity and heat flow fields, *Chin. Sci. Bull.*, **46**, 596–599.

Hall, R.T., Bendfeldt, P., Obee,T.N. and Sangiovanni, J.J. (1998) Computational and experimental studies of UV/titania photocatalytic oxidation of VOCs in honeycomb monoliths, *J. Adv. Oxidation Technol.*, **3**, 243–251.

Haymore, C. and Odom, R. (1993) Economic effects of poor IAQ, *EPA J.*, **19**, 28–29.

Hossain, Md.M, Gregory, B.R., Hay, S.O. and Obee, T.N. (1999) Three-dimensional developing flow model for photocatalytic monolith reactors, *AIChE J.*, **45**, 1309–1321.

Kim, Y.M., Harrad, S. and Harrison, R.M. (2001) Concentrations and sources of VOCs in urban domestic and public microenvironments, *Environ. Sci. Technol.*, **35**, 997–1004.

Meininghaus, R., Salthammer, T. and Knoppel, H. (1999) Interaction of volatile organic compounds with indoor materials – a small-scale screening method, *Atmos. Environ.*, **33**, 2395–2401.

Molhave, L. (1989) The sick buildings and other buildings with indoor climate problems, *Environ. Int.*, **15**, 65–74.

Obee, T.N and Brown, R.T. (1995) TiO_2 photocatalysis for indoor air applications: effects of humidity and trace concentration levels on the oxidation rates of formaldehyde, toluene and 1, 3 –butadiene, *Environ. Sci. Technol.*, **29**, 1223–1231.

Obee, T.N. (1996) Photooxidation of sub-parts-per-million toluene and formaldehyde levels on titania using a glass-plate reactor, *Environ. Sci. Technol.*, **30**, 3578–3584.

Obee, T.N. and Hay, S.O. (1997) Effect of moisture and temperature on the photooxidation of ethylene on titania, *Environ. Sci. Technol.*, **31**, 2034–2038.

Tao, W.Q., Guo, Z.Y. and Wang, B.X. (2002) Field synergy principle for enhancing convective heat transfer–its extension and numerical verifications, *Int. J. Heat Mass Transfer*, **45**, 3849–3856.

Tao, W.Q., He, Y.L. and Wang, Q.W. (2002) A unified analysis on enhancing single phase convective heat transfer with field synergy principle, *Int. J. Heat Mass Transfer*, **45**, 4871–4879.

Tompkins, D.T. (2002) Evaluation of photocatalytic air cleaning capability: a literature review and engineering analysis, ASHARE Research Project RP-1134.

Tronconi, E. and Forzatti, P. (1992) Adequacy of lumped parameter models for SCR reactors with monolith structure, *AIChE J.*, **38**, 201–210.

US EPA (1990) *Reducing Risk: Setting Priorities and Strategies for Environmental Protection*, Washington D.C., US Environmental Protection Agency.

WHO (1989) Indoor air quality: organic pollutants*EURO Report and Studies*ol. 3, Copenhagen, WHO Regional Office for Europe.

Yang, R. and Zhang, Y.P. (2004) An improved model for analyzing the performance of photocatalytic oxidation reactor in removing volatile organic compounds and its application, *J. Air Waste Manage. Assoc.*, **54**, 1516–1524.

Yoneyama, H. and Torimoto, T. (2000) Titanium dioxide/adsorbent hybrid photocatalysts for photodestruction of organic substances of dilute concentrations, *Catal. Today*, **58**, 133–140.

Zhang, Y.P., Yang, R. and Zhao, R.Y. (2003) A model for analyzing the performance of photocatalytic air cleaner in removing volatile organic compounds. *Atmos. Environ.*, **37**, 3395–3399.